

A Comparison of Optical Properties of CuO and Cu₂O Thin Films for Solar Cell Applications

Radu Bunea, Ashwin Kumar Saikumar, Kalpathy Sundaram

University of Central Florida, Orlando, USA

Email: rbunea@valenciacollege.edu

How to cite this paper: Bunea, R., Saikumar, A.K. and Sundaram, K. (2021) A Comparison of Optical Properties of CuO and Cu₂O Thin Films for Solar Cell Applications. *Materials Sciences and Applications*, 12, 315-329.

<https://doi.org/10.4236/msa.2021.127021>

Received: May 5, 2021

Accepted: June 29, 2021

Published: July 2, 2021

Copyright © 2021 by author(s) and Scientific Research Publishing Inc.

This work is licensed under the Creative Commons Attribution International License (CC BY 4.0).

<http://creativecommons.org/licenses/by/4.0/>



Open Access

Abstract

Solar energy is becoming more popular and widespread, and consequently, the materials to manufacture solar cells are becoming more limited and costly. Therefore, in order to keep solar energy affordable and available, we must research alternative materials such as copper oxides. Some benefits of copper oxides include being available in abundance, affordable, low toxicity, low bandgap, and a high absorption coefficient—all of which contribute to it being a valuable interest for the manufacturing of solar cells. In this study, CuO thin films were synthesized utilizing RF sputtering technique with deposition occurring at room temperature followed by thermal annealing between 100°C and 400°C and using different gases, oxygen (O₂) (oxidizing and reactive gas) and nitrogen (N₂) (inert gas), besides air. Afterwards, these thin films were evaluated for a range of wavelengths: 200 - 400 nm (UV spectrum), 400 - 700 nm (Visible spectrum), and 700 - 800 nm (IR spectrum), for both, optical transmittance and photoluminescence. In addition, the CuO results were compared to our Cu₂O results from a previous study to assess their differences. In the results of this study, the CuO thin film initially had a bandgap of 2.19 eV at room temperature, and by increasing the annealing temperature to different levels, the bandgap decreased respectively. The presence of air in the chamber allowed for the highest decrease, followed by the nitrogen (N₂) and the lowest decrease was observed in the presence of oxygen (O₂). This was reflected in the decrease in the bandgap values from 2.19 eV (room temperature) to 2.05 eV for the films annealed at 400°C.

Keywords

Cu₂O Thin Film, Cuo Thin Film, Optical Properties, Bandgap, Photoluminescence

1. Introduction

The current materials used to manufacture photovoltaics are becoming scarce,

and as a result, expensive. A solution will be to investigate other materials that might qualify to fill the gap and be used as replacements. Metal oxides are one of these materials that are readily available and currently have a low cost of manufacturing [1]. In addition, copper oxides also have low toxicity, low bandgap, and a high absorption coefficient which are all valuable qualities. The most popular forms of copper oxides include the following: cupric oxide (CuO—tenorite in the mineral form), cuprous oxide (Cu₂O), and Cu₄O₃ (paramelaconite in the mineral form) [2]. The paramelaconite is a meta-stable copper oxide, which is an intermediate compound between CuO and Cu₂O. The stable forms are the CuO and the Cu₂O. Both show promising qualities due to their electrical and optical properties [3]. The CuO has a dark brown/black color and the Cu₂O is a yellow/red color [2]. In the presence of moist air, the Cu₂O will change into CuO. The CuO has a smaller bandgap than Cu₂O and as a result, is potentially superior in photon-detection and optical switching applications that are used in combination with visible and near-infrared spectrums [4]. The Cu₂O has a cubic structure and a bandgap between 2.0 eV and 2.6 eV [5]. The CuO has a monoclinic (a group of crystalline solids whose crystals have three axes of unequal length, with two being perpendicular to one another) structure with a bandgap between 1.3 eV and 2.2 eV [5]. In theory, a material qualifies for solar applications if it has good absorption of solar radiation ($\alpha = 1$) in the visible (400 nm to 700 nm) and near-infrared spectrum (700 nm to 2000 nm), and no emission ($\varepsilon = 0$) in the infrared region (2000 nm to 20,000 nm) [5].

Cupric oxide (CuO) is potentially a good candidate for solar cell applications due to high electron mobility and high optical absorptivity in the visible spectrum [1]. It also has high conductivity and low electrical resistivity. The copper oxides are p-type semiconductors and are usually coupled with n-type semiconductors like zinc oxide (ZnO), silicon (Si), and cadmium sulfide (CdS) [4]. The high conduction of the p-type copper oxide is attributed mainly to the negatively charged copper (Cu) vacancies [5]. Application-wise, besides solar cells, copper oxides are utilized in lithium-ion batteries, photocatalysts, and photoelectron-chemical cells [6]. Currently, there are a few different methods to produce copper oxide thin films like reactive sputtering, anodizing, chemical conversion, chemical vapor deposition, and thermal oxidization [6]. Sputtering is an inexpensive method of creating copper oxide thin films. In addition, other characteristics of this method are the high deposition rate, dense layer formation, good surface flatness, and low substrate temperature [7].

CuO and Cu₂O were both investigated as a result of having different properties that could contribute to their effectiveness in solar cell applications. CuO is more thermally stable when compared to Cu₂O, and this is due to having a high oxidation number [8]. This is beneficial because one of the current issues with solar cells is that they can overheat which in turn causes them to conduct less; utilizing a more thermal stable element can help to circumvent this issue. On the other hand, Cu₂O has relatively higher hole transport properties when compared

to CuO [9]. This is beneficial because it becomes easier to induce electron flow, which means better efficiency. Therefore, both of these metal oxides show promising qualities and deserve equal investigation to understand which could be the future of solar cells.

2. Experimental Procedure

The methodology for both the CuO thin films and Cu₂O thin films were identical. Briefly, the thin films were deposited on glass slides using RF magnetron sputtering technique via an in-house built sputtering system. Argon was utilized as the only sputtering gas while deposition occurred at room temperature. The following parameters remained constant for all films: base pressure (4×10^{-5} Torr), thickness (2000 Angstrom), RF power (10 standard cubic centimeters per minute), Argon flow (10 mTorr), and chamber pressure (50 W).

Three sets of each type of thin film were made by systematically annealing for thirty minutes in an isotemp programmable muffle furnace at temperatures of 100°C to 400°C in the presence of oxygen (O₂), nitrogen (N₂) and air respectively [10]. The annealing furnace gas flow was also constant at 100 standard cubic centimeters per minute (SCCM). Afterwards, both optical transmissions and photoluminescence measurements were recorded for each thin film.

In addition, both the Tauc plot method and the photoluminescence (PL) method were utilized for calculating the optical bandgap values.

The Tauc plot method entails utilizing the absorption coefficient of the thin film, calculated by Equation (1), and then the Tauc plot was graphed by fitting this data into Equation (2) [10].

$$\alpha_{\lambda} = \frac{-\ln(T)}{t} \quad (1)$$

$$(\alpha_{\lambda} \cdot hv)^2 = B(hv - E_g) \quad (2)$$

where α_{λ} = absorption coefficient, T = optical transmission, t = thickness of film, hv = photon energy, B = constant factor, and E_g = optical bandgap.

The PL method entails utilizing wavelengths obtained from the excitation curve (PL peaks) and fitting that data into Equation (3) to calculate the bandgap values.

$$E_g = h \cdot \nu = h \cdot \frac{c}{\lambda} \quad (3)$$

where h = Planck's constant = 4.135×10^{-15} eV·s, c = speed of light in vacuum = 3×10^8 m/s, and λ = wavelength.

For full details of methodology, see R. Bunea *et al.* 2021 [10].

3. Results and Discussion

As a result of annealing temperature, the levels of transparency differed between each type of thin film: semi-transparent at room temperature, and near opaque at higher temperatures (400°C). Overall, each of the thin films had a strong ab-

sorption in the UV region (200 nm - 400 nm). The following figures show the optical transmission spectrums for the CuO thin films annealed in three different mediums: air, oxygen, and nitrogen. For the optical transmission results for Cu₂O thin films, see R. Bunea *et al.* 2021 [10].

Figure 1 shows the first series of CuO thin films annealed in air.

For the CuO thin films annealed in air (**Figure 1**), maximum transmission was 82.51% at 800 nm for room temperature, and 69.65% at 800 nm for high temperature (400°C). However, at the optical bandgap (566 nm), maximum transmission was 34.30% for room temperature, and 22.14% for high temperature (400°C).

Figure 2 shows the second series of CuO thin films annealed in oxygen (O₂).

For the CuO thin films annealed in oxygen (**Figure 2**), maximum transmission was 82.51% at 800 nm for room temperature, and 71.69% at 800 nm for high temperature (400°C). However, at the optical bandgap (566 nm), maximum transmission was 34.30% for room temperature, and 24.57% for high temperature (400°C).

Figure 3 shows the third series of CuO thin films annealed in nitrogen (N₂).

For the CuO thin films annealed in nitrogen (**Figure 3**), maximum transmission was 82.51% at 800 nm for room temperature, and 71.57% at 800 nm for high temperature (400°C). However, at the optical bandgap (566 nm), maximum transmission was 34.30% for room temperature, and 24.95% for high temperature (400°C).

Overall, there was a common trend among **Figure 1** through **Figure 3**: as the annealing temperature increased, the optical transmission decreased, and this was observed at the optical bandgap (566 nm) especially. Therefore, the conclusion

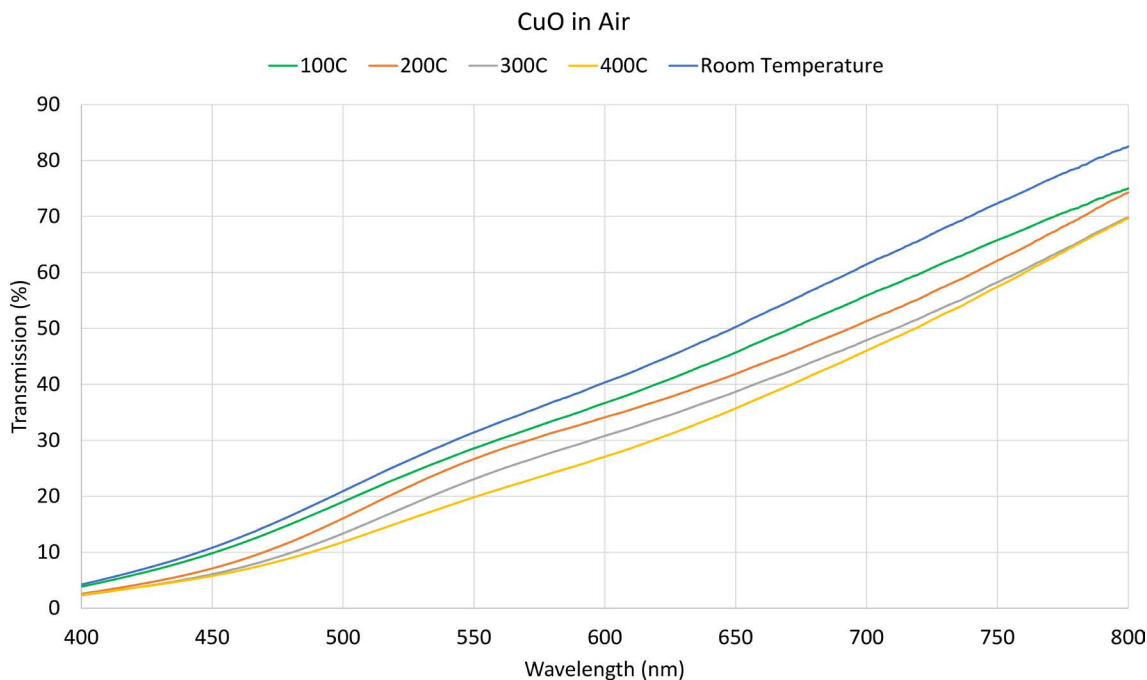


Figure 1. Transmission spectra of CuO thin films annealed in air.

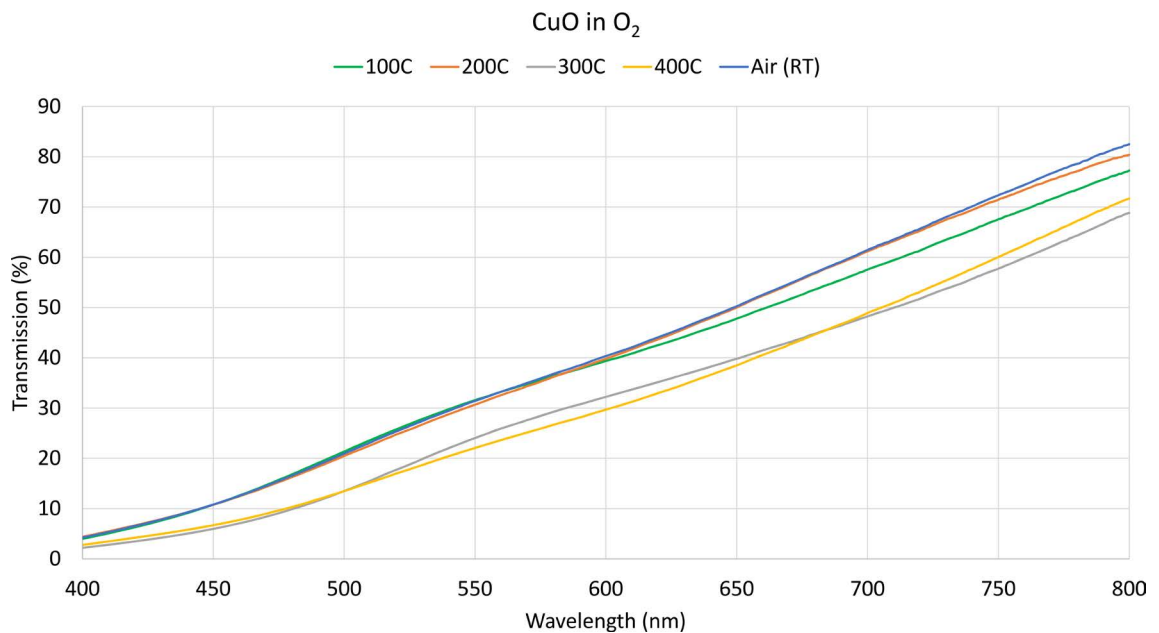


Figure 2. Transmission spectra of CuO thin films annealed in O₂ reactive gas.

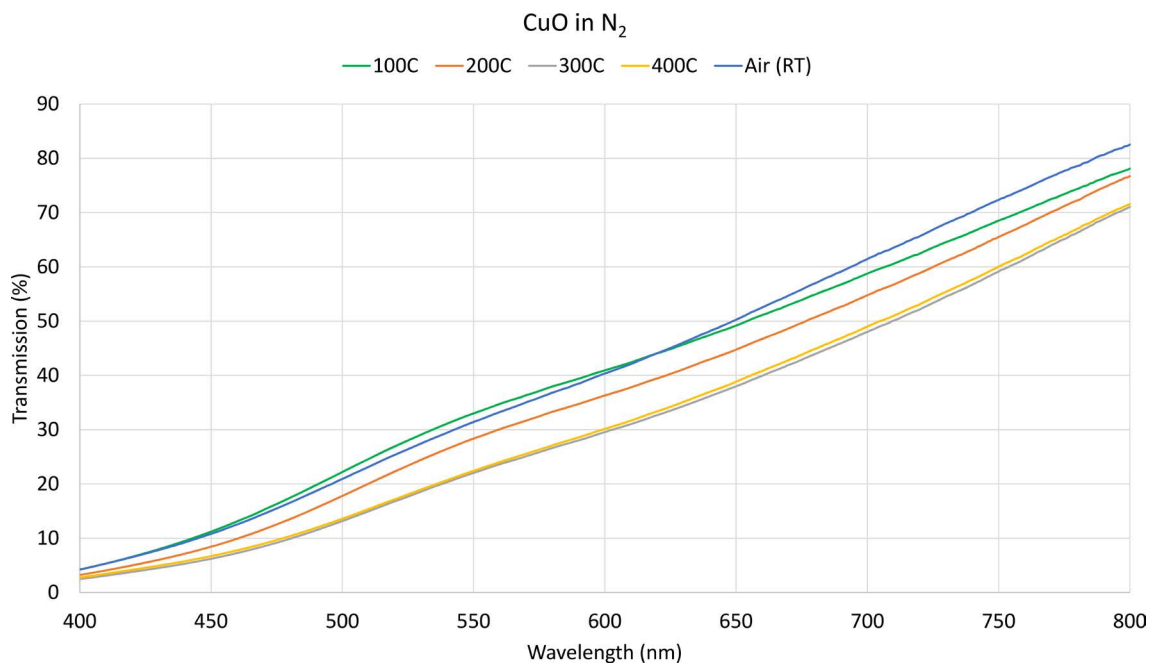


Figure 3. Transmission spectra of CuO thin films annealed in N₂ inert gas.

is that the transmission varies as a function of annealing temperature, and the above results show evidence of an inversely proportional relationship between these two variables.

Table 1 summarizes the optical transmission values obtained at different temperatures.

As seen in R. Bunea *et al.* 2021, the absorption coefficients were calculated from the transmission data using Equation (1), and these results were then used to determine the bandgap values using Equation (2) (Tauc plot method) [10].

Figure 4 through Figure 8 show the Tauc plot for the absorption coefficient for CuO, ranging from room temperature to 400°C.

Table 2 summarizes the bandgap energy values obtained at different temperatures.

Rearranging Equation (1) will allow for the calculation of the wavelength from the bandgap energy determined using the Tauc method [10].

$$E_g = h \cdot \nu = h \cdot \frac{c}{\lambda} \rightarrow \lambda = h \cdot \frac{c}{E_g} \tag{4}$$

where h = Planck’s constant = 4.135×10^{-15} eV·s, c = speed of light in vacuum = 3×10^8 m/s, and λ = wavelength.

Table 3 summarizes the calculated wavelength values.

Figure 9 through Figure 13 show the photoluminescence measurements for

Table 1. CuO Thin Films optical transmission results.

Annealing Medium	Wavelength	CuO Thin Films Transmission				
		RT (no annealing)	100°C	200°C	300°C	400°C
Air			75.01%	74.27%	69.83%	69.65%
O ₂	800 nm (IR)	82.51%	77.26%	80.38%	68.85%	71.69%
N ₂			78.10%	76.72%	71.04%	71.57%
Air			31.18%	29.27%	25.73%	22.14%
O ₂	566 nm (VIS)	34.30%	34.18%	33.62%	26.94%	24.57%
N ₂			35.71%	31.06%	24.51%	24.95%

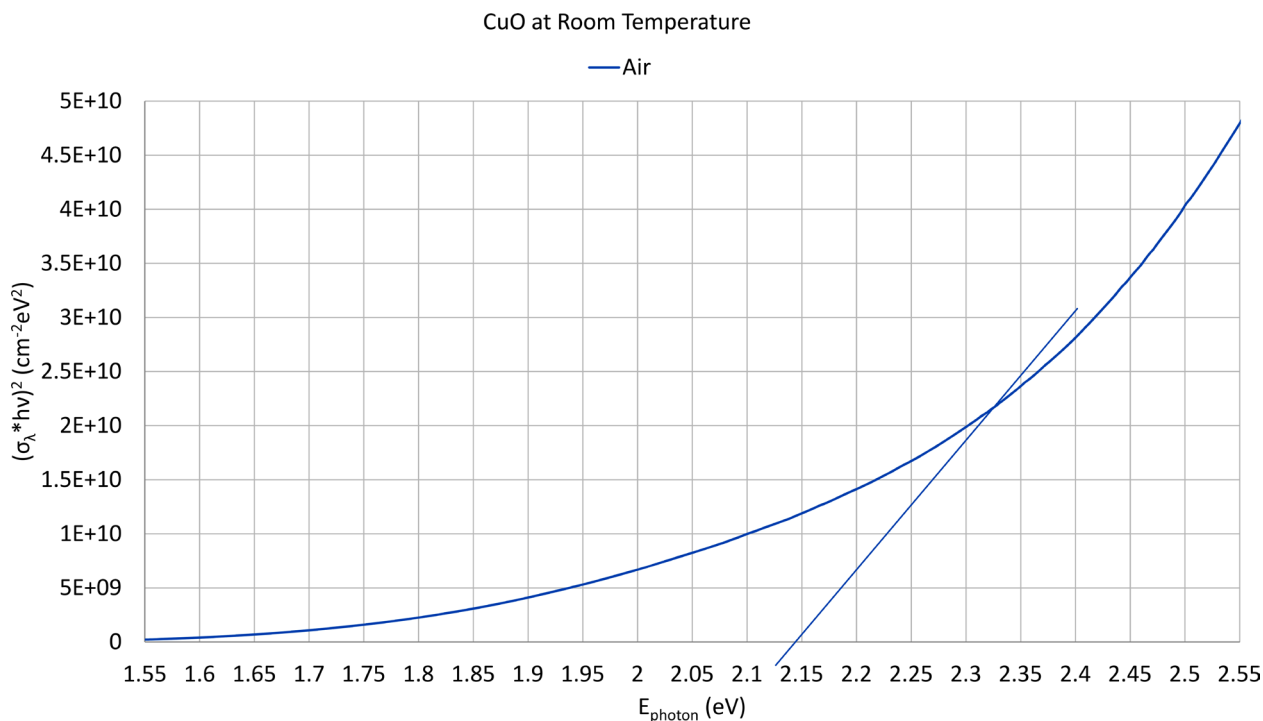


Figure 4. CuO thin film optical bandgap (room temperature).

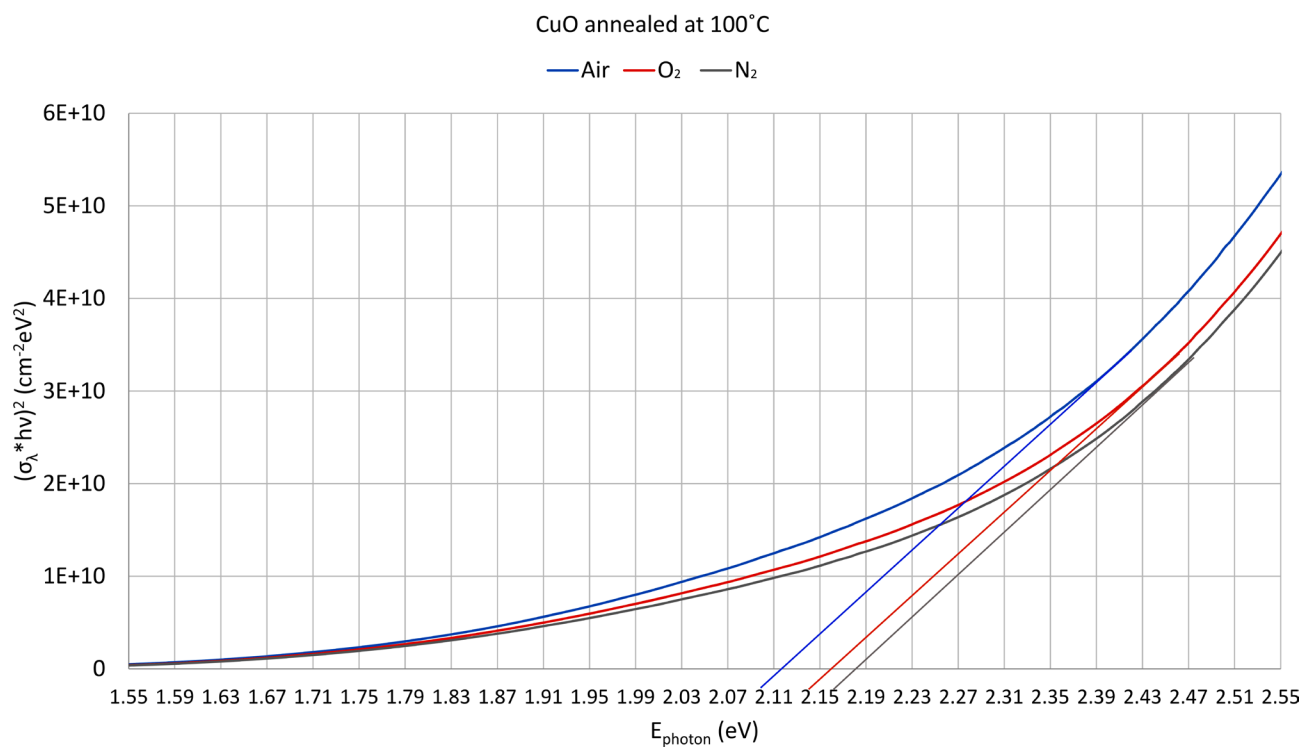


Figure 5. CuO thin films optical bandgap (annealed at 100°C).

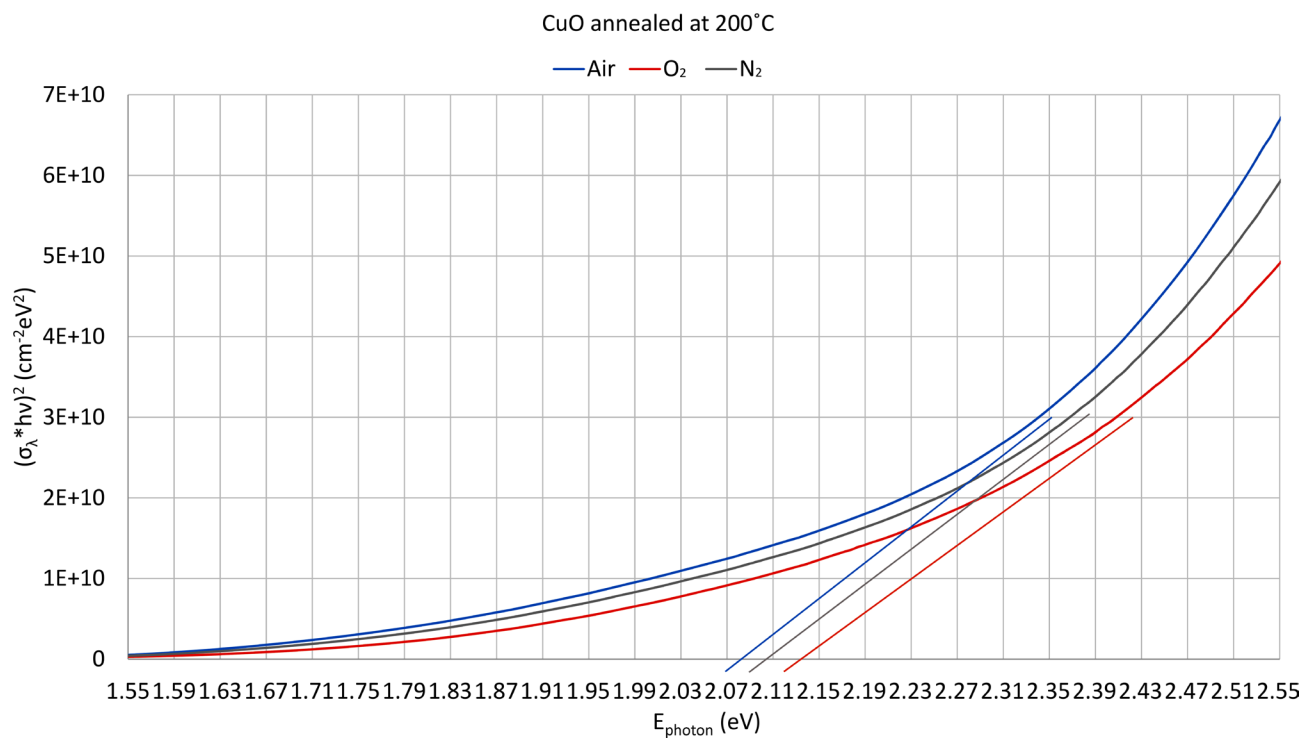


Figure 6. CuO thin films optical bandgap (annealed at 200°C).

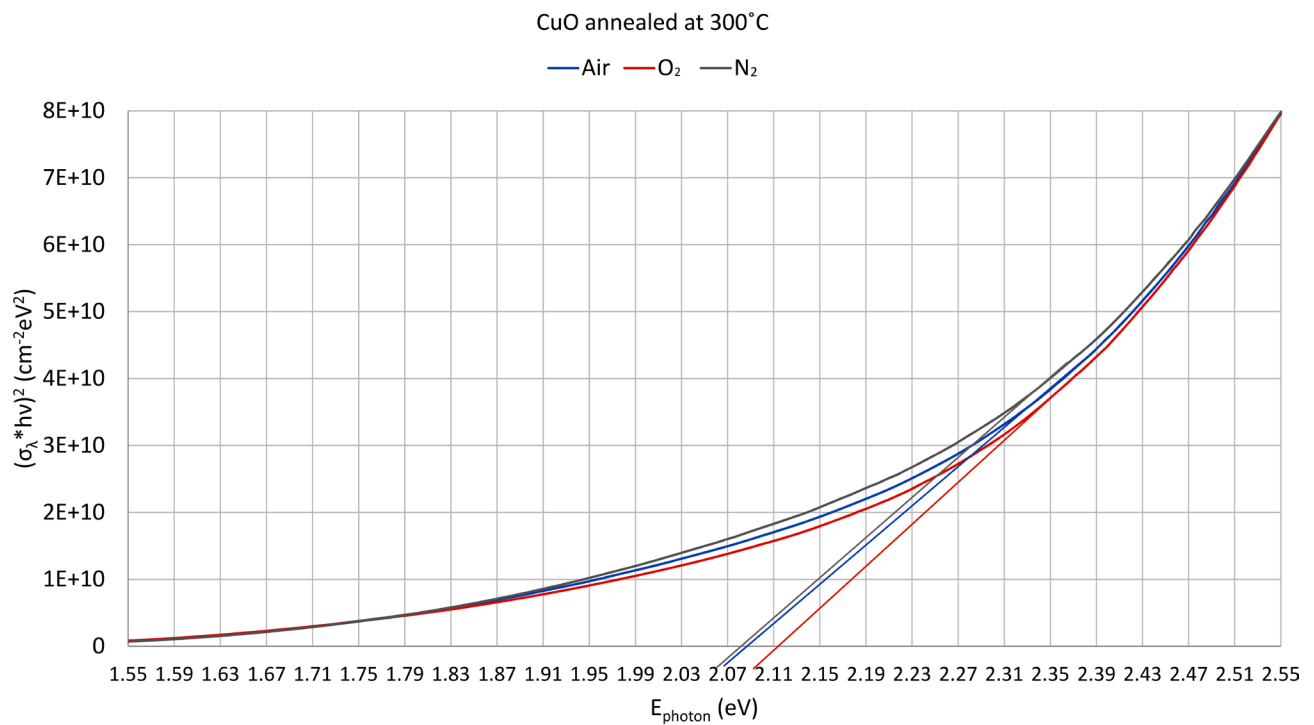


Figure 7. CuO thin films optical bandgap (annealed at 300°C).

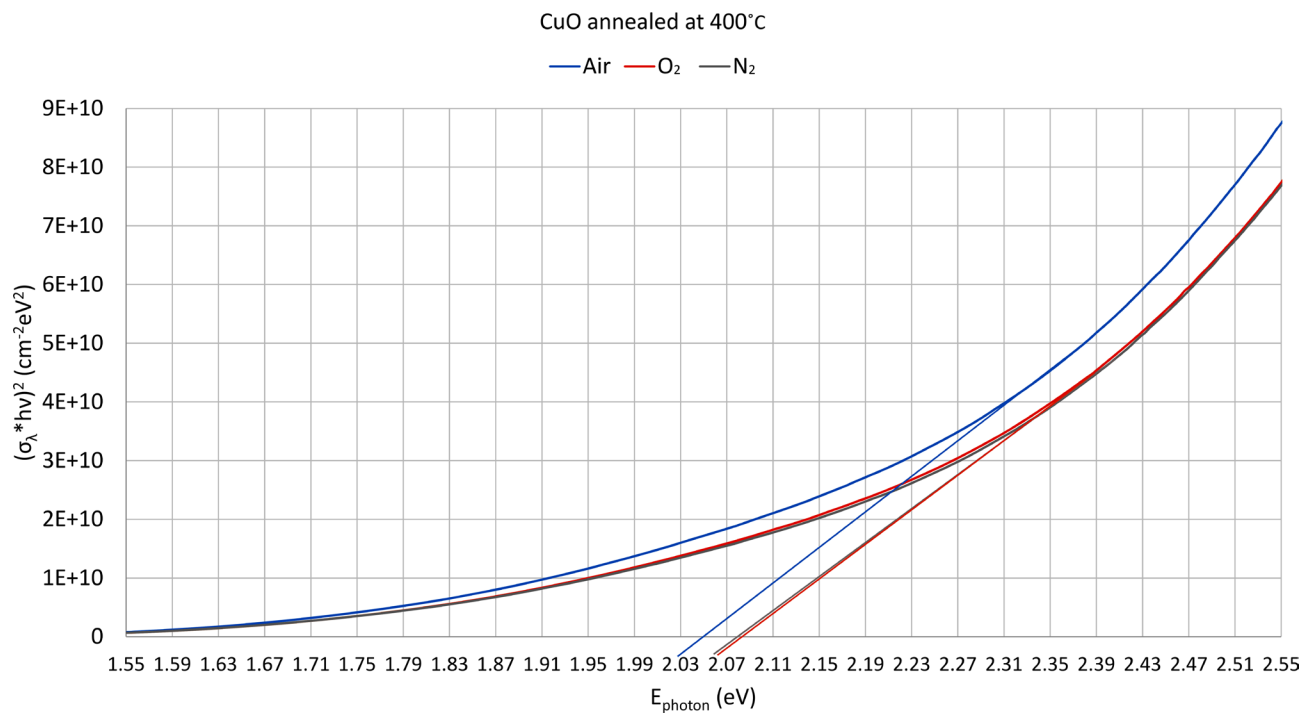


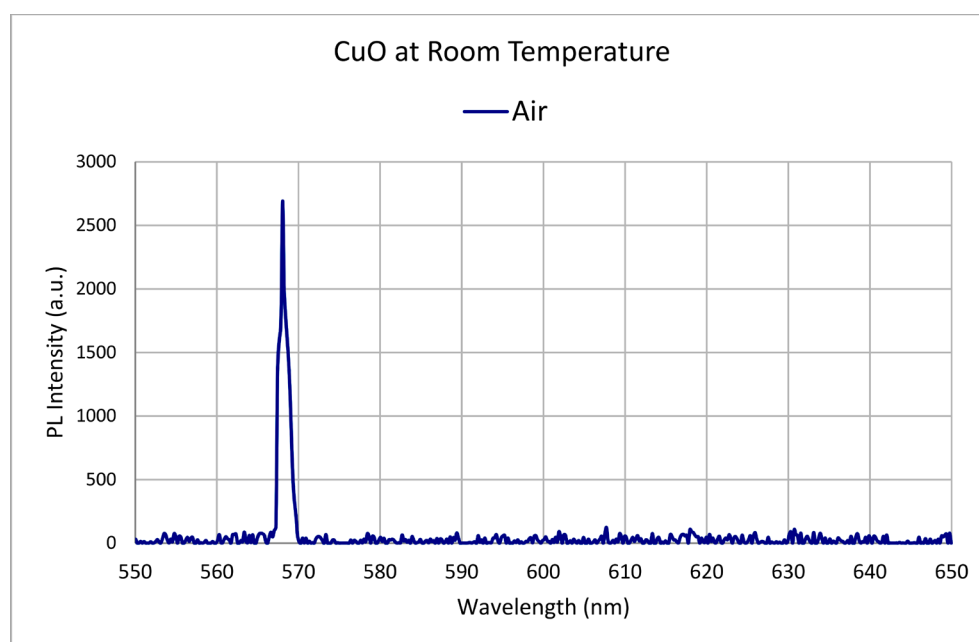
Figure 8. CuO thin films optical bandgap (annealed at 400°C).

Table 2. CuO thin films optical bandgap values (Tauc plot method).

CuO Thin Films			
Temperature	Optical Bandgap (Tauc)		
	Air	O ₂	N ₂
Room Temperature		2.19 eV	
100 °C	2.12 eV	2.16 eV	2.17 eV
200 °C	2.09 eV	2.13 eV	2.10 eV
300 °C	2.08 eV	2.11 eV	2.09 eV
400 °C	2.05 eV	2.09 eV	2.08 eV

Table 3. CuO wavelength peaks (Tauc plot method).

CuO Thin Films			
Temperature	Wavelength (Tauc)		
	Air	O ₂	N ₂
Room Temperature		566 nm	
100 °C	585 nm	574 nm	571 nm
200 °C	593 nm	582 nm	590 nm
300 °C	596 nm	588 nm	593 nm
400 °C	605 nm	593 nm	596 nm

**Figure 9.** PL Spectra of CuO thin film (room temperature).

CuO, ranging from room temperature to 400 °C.

Using the spectrometer software, the following specs were adjusted: integration time of 400 ms and reference spectrum stored as a background spectrum.

Table 4 shows the PL peaks results observed.

Utilizing Equation (3) will allow for the calculation of the bandgap energy from the PL peaks measured.

Table 5 summarizes the calculated bandgap energy values.

Overall, there was a perceptible difference in the effect that altering the annealing temperature had, and there was a shift between mediums evident for both types of thin films. The Cu₂O thin films showed a shift from a lower spectrum peak (478 nm) for the thin film created in air, to 483 nm at 100°C and all

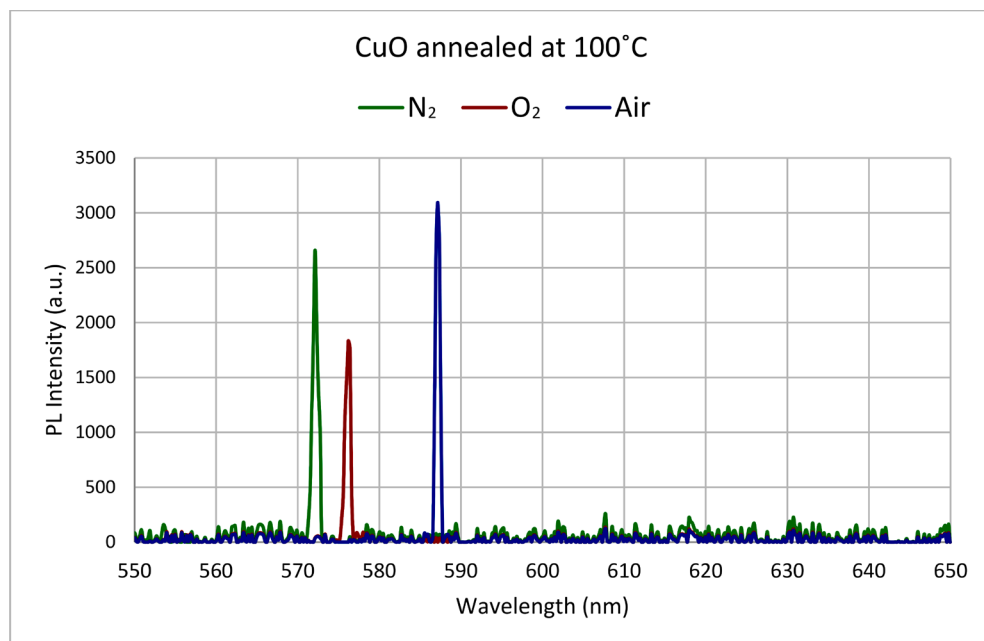


Figure 10. PL Spectra of CuO thin films (annealed at 100°C).

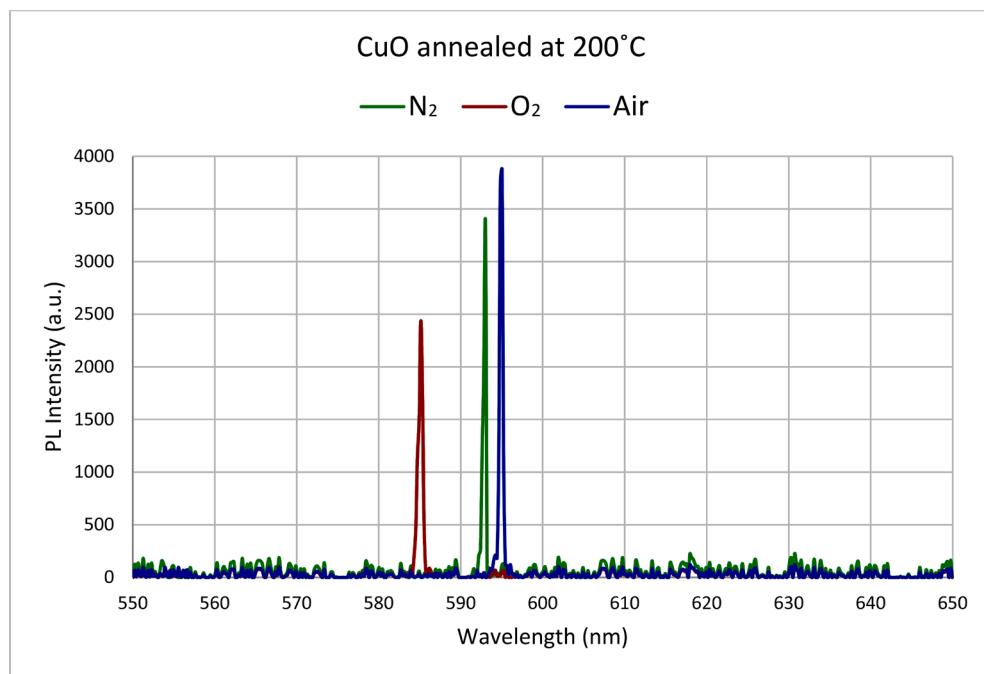


Figure 11. PL Spectra of CuO thin films (annealed at 200°C).

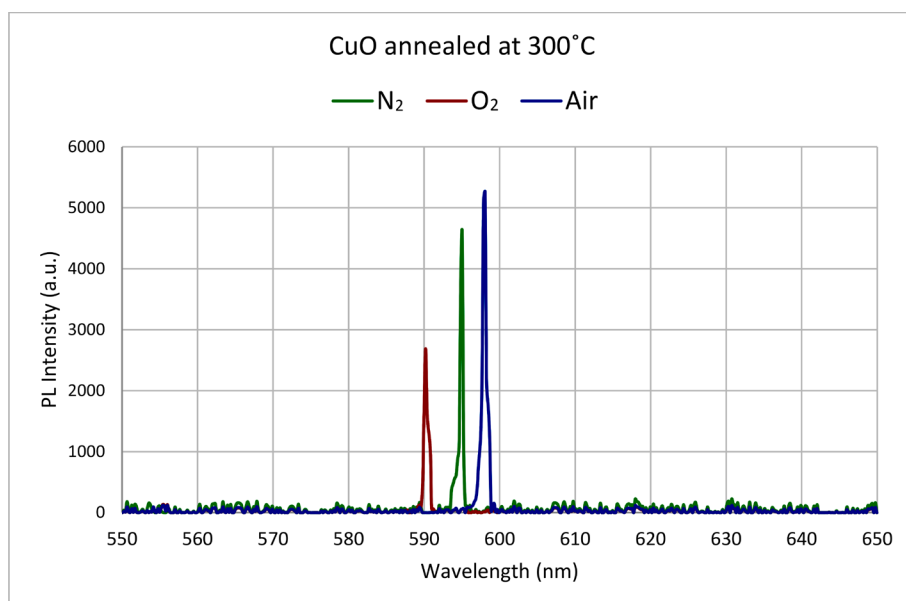


Figure 12. PL Spectra of CuO thin films (annealed at 300°C).

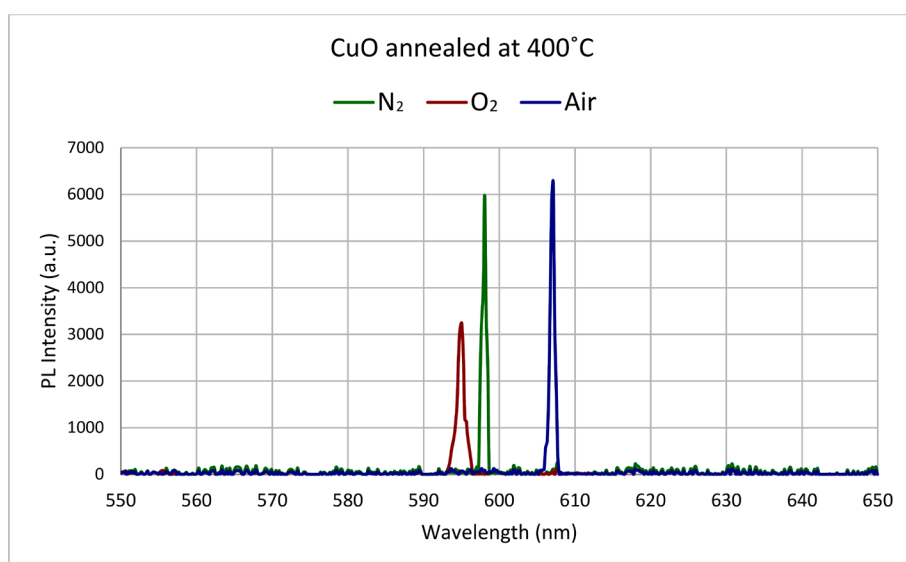


Figure 13. PL Spectra of CuO thin films (annealed at 400°C).

Table 4. CuO thin films wavelength peaks (PL method).

CuO Thin Films			
Temperature	Wavelength (PL)		
	Air	O ₂	N ₂
Room Temperature		568 nm	
100°C	587 nm	576 nm	572 nm
200°C	595 nm	585 nm	593 nm
300°C	598 nm	590 nm	595 nm
400°C	607 nm	595 nm	598 nm

Table 5. CuO thin films optical bandgap values (PL method).

CuO Thin Films			
Temperature	Optical Bandgap (PL)		
	Air	O ₂	N ₂
Room Temperature		2.18 eV	
100°C	2.11 eV	2.15 eV	2.16 eV
200°C	2.08 eV	2.11 eV	2.09 eV
300°C	2.07 eV	2.10 eV	2.08 eV
400°C	2.04 eV	2.08 eV	2.07 eV

the way to 550 nm at 400°C for the film annealed in nitrogen (N₂) [10]. The CuO thin films showed a shift from a lower spectrum peak (568 nm) for the thin film created in air, to 587 nm at 100°C and all the way to 607 nm at 400°C for the film annealed in air. The thin film annealed in nitrogen (N₂) at 400°C created a peak at 598 nm. If the annealing temperature is increased even higher than 400°C, an even higher PL peak for the CuO thin films can be achieved, which will transition the output spectrum to upper visible and even infrared [10]. However, the increase in annealing temperature will require upgrading the thin films substrate from glass to a metal due to the fact that the annealing temperature for a microscope glass slide is 545°C and its softening temperature is 724°C (according to the microscope slides manufacturer). This change will also affect the budget for the experiment due to the price differences between the different substrates. The increase in the annealing temperature induces the formation of a more hard packed structure, and the sharper peaks obtained for the thin films annealed at 400°C indicate a higher uniformity of the composition and strain [10].

The next step is to look at how utilizing either the Tauc plot method or photoluminescence (PL) method can affect the wavelength and bandgap energy levels. In order to use the Tauc method, first the transmittance must be obtained and then the absorption coefficient can be calculated from that value. Then, the Tauc method relates absorption coefficient to photon energy to calculate the bandgap energy. Only then can the wavelength be calculated from bandgap energy utilizing Equation (1). On the other hand, using the PL method, the wavelength can be obtained from the excitation curve, and then the bandgap energy can be calculated utilizing Equation (2).

Table 6 summarizes the optical bandgap values as they are calculated by the Tauc plot method and PL measurements, for both types of thin films.

When evaluating bandgap, there is a common trend among these values—when comparing the two methods, the bandgap values decrease from Tauc plot method to PL method.

Table 7 summarizes the wavelength values as they are calculated by the Tauc plot method and PL measurements, for both types of thin films.

Table 6. Comparison of Cu₂O and CuO thin films optical bandgap values (Tauc and PL method).

Bandgap						
Cuprous Oxide (Cu ₂ O)						
Temperature	Tauc			PL		
	Air	O ₂	N ₂	Air	O ₂	N ₂
Room Temperature	2.58 eV			2.56 eV		
100 °C	2.53 eV	2.55 eV	2.54 eV	2.51 eV	2.53 eV	2.52 eV
200 °C	2.47 eV	2.53 eV	2.48 eV	2.45 eV	2.51 eV	2.46 eV
300 °C	2.26 eV	2.29 eV	2.28 eV	2.24 eV	2.27 eV	2.26 eV
400 °C	2.21 eV	2.22 eV	2.17 eV	2.20 eV	2.20 eV	2.15 eV
Cupric Oxide (CuO)						
Temperature	Tauc			PL		
	Air	O ₂	N ₂	Air	O ₂	N ₂
Room Temperature	2.19 eV			2.18 eV		
100 °C	2.12 eV	2.16 eV	2.17 eV	2.11 eV	2.15 eV	2.16 eV
200 °C	2.09 eV	2.13 eV	2.10 eV	2.08 eV	2.11 eV	2.09 eV
300 °C	2.08 eV	2.11 eV	2.09 eV	2.07 eV	2.10 eV	2.08 eV
400 °C	2.05 eV	2.09 eV	2.08 eV	2.04 eV	2.08 eV	2.07 eV

Table 7. Comparison of Cu₂O and CuO thin films wavelength values (Tauc and PL method).

Wavelength						
Cuprous Oxide (Cu ₂ O)						
Temperature	Tauc			PL		
	Air	O ₂	N ₂	Air	O ₂	N ₂
Room Temperature	480 nm			484 nm		
100 °C	490 nm	486 nm	488 nm	494 nm	490 nm	492 nm
200 °C	502 nm	490 nm	500 nm	506 nm	494 nm	504 nm
300 °C	548 nm	541 nm	544 nm	553 nm	546 nm	548 nm
400 °C	561 nm	558 nm	571 nm	564 nm	563 nm	578 nm
Cupric Oxide (CuO)						
Temperature	Tauc			PL		
	Air	O ₂	N ₂	Air	O ₂	N ₂
Room Temperature	566 nm			568 nm		
100 °C	585 nm	574 nm	571 nm	587 nm	576 nm	572 nm
200 °C	593 nm	582 nm	590 nm	595 nm	585 nm	593 nm
300 °C	596 nm	588 nm	593 nm	598 nm	590 nm	595 nm
400 °C	605 nm	593 nm	596 nm	607 nm	595 nm	598 nm

When evaluating wavelength, once again there is a common trend among these values as well—when comparing the two methods, the wavelength values increase from Tauc method to PL method.

Both the bandgap and wavelength can be calculated from either method, however, they will still result in different values. Specifically, the difference in bandgaps between the Tauc and PL methods is due to the red shift in wavelength in PL—in turn, this is because of a trap state present in which nonradiative decay of the photon occurs [11]. The red shift in PL means an increase in wavelength which indicates a decrease in energy. Hence, the lower bandgap energy observed when calculated via the PL method in **Table 6**, and the higher wavelength in **Table 7**.

4. Conclusions

In this study, the optical properties of CuO thin films were investigated and compared to the Cu₂O thin films from our previous work. The optical bandgap for CuO thin films varied between 2.19 eV (room temperature) to 2.05 eV (400°C in air), and for Cu₂O thin films, it varied between 2.58 eV (room temperature) to 2.17 eV (400°C in N₂). Both thin films show promising capabilities for photovoltaic solar conversion applications. A solar semiconductor should have an overall bandgap between 1.00 eV and 1.70 eV to be considered effective. Therefore, a future study could include identifying which n-type semiconductors work best in conjunction with these copper oxides in order to produce the lowest possible bandgap within the proper range for solar cell use.

In addition, when looking at the various gases introduced in the annealing chamber for CuO thin films, it was observed that oxygen (O₂) had a minor effect, while the regular atmosphere (air) or nitrogen (N₂) created the largest impact. However, for the Cu₂O thin films, nitrogen alone had the largest impact while air and oxygen had minor impacts. Therefore, another future study could include a characterization of nitrogen-doped (N-doped) cupric oxide (CuO) for solar cell applications.

Conflicts of Interest

The authors declare no conflicts of interest regarding the publication of this paper.

References

- [1] Ahmmed, S., Aktar, A., Tabassum, S., Rahman, Md.H., Rahman, Md.F. and Ismail, A.B.Md. (2021) CuO Based Solar Cell with V₂O₅ BSF Layer: Theoretical Validation of Experimental data. *Superlattices and Microstructures*, **151**, Article No. 106830. <https://doi.org/10.1016/j.spmi.2021.106830>
- [2] Guillén, C. and Herrero, J. (2018) Single-Phase Cu₂O and CuO Thin Films Obtained by Low-Temperature Oxidation Processes. *Journal of Alloys and Compounds*, **737**, 718-724. <https://doi.org/10.1016/j.jallcom.2017.12.174>
- [3] Sultana, J., Paul, S., Saha, R., Sikdar, S., Karmakar, A. and Chattopadhyay, S. (2020)

- Optical and Electronic Properties of Chemical Bath Deposited p-CuO and n-ZnO Nanowires on Silicon Substrates: p-CuO/n-ZnO Nanowires Solar Cells with High Open-Circuit Voltage and Short-Circuit Current. *Thin Solid Films*, **699**, Article No. 137861. <https://doi.org/10.1016/j.tsf.2020.137861>
- [4] Ajili, M. and Kamoun, N.T. (2021) Structural and Optoelectronic Studies of CuO, $\text{In}_{2-x}\text{Al}_x\text{S}_3$ and $\text{SnO}_2\text{:F}$ sprayed thin films for solar cell application: Au/CuO (p)/ $\text{In}_{2-x}\text{Al}_x\text{S}_3$ (n)/ $\text{SnO}_2\text{:F}$. *Optik*, **229**, Article No. 166222. <https://doi.org/10.1016/j.ijleo.2020.166222>
- [5] Shabu, R., Moses Ezhil Raj, A., Sanjeeviraja, C. and Ravidhas, C. (2015) Assessment of CuO Thin Films for Its Suitability as Window Absorbing Layer in Solar Cell Fabrications. *Materials Research Bulletin*, **68**, 1-8. <https://doi.org/10.1016/j.materresbull.2015.03.016>
- [6] David Prabu, R., Valanarasu, S., Ganesh, V., Shkir, M., Kathalingam, A. and AlFai-fy, S. (2018) Effect of Spray Pressure on Optical, Electrical and Solar Cell Efficiency of Novel Cu_2O Thin Films. *Surface and Coatings Technology*, **347**, 164-172. <https://doi.org/10.1016/j.surfcoat.2018.04.084>
- [7] Raebiger, H., Lany, S. and Zunger, A. (2007) Origins of the *p*-Type Nature and Cation Deficiency in Cu_2O and Related Materials. *Physical Review B*, **76**, Article No. 045209. <https://doi.org/10.1103/PhysRevB.76.045209>
- [8] Raship, N.A., Sahdan, M.Z., Adriyanto, F., Nurfazliana, M.F. and Bakri, A.S. (2017) Effect of annealing temperature on the properties of copper oxide films prepared by dip coating technique. *AIP Conference Proceedings*, **1788**, Article No. 030121. <https://doi.org/10.1063/1.4968374>
- [9] Ahn, S.-Y., Park, K., Choi, D., Park, J., Kim, Y.J. and Kim, H.-S. (2019) A Study on the Transition of Copper Oxide by the Incorporation of Nitrogen. *Electronics*, **8**, Article No. 1099. <https://doi.org/10.3390/electronics8101099>
- [10] Bunea, R., Saikumar, A. and Sundaram, K. (2021) The Effect of Annealing Temperature and Reactive Gases on Optical Properties of Cu_2O Thin Films. *Materials Sciences and Applications*, **12**, 182-196. <https://doi.org/10.4236/msa.2021.125012>
- [11] Baruah, R. (n.d.) Study of Optical Absorption and Photoluminescence (PL) of Hexa Thiobenzene Acid. Indian Academy of Sciences. <http://reports.ias.ac.in/report/20872/study-of-optical-absorption-and-photoluminescence-pl-of-hexa-thiobenzene-acid>